This is the accepted manuscript made available via CHORUS. The article has been published as:

Coupled fission fragment angular momenta

Jørgen Randrup

Phys. Rev. C **106**, L051601 — Published 17 November 2022

DOI: 10.1103/PhysRevC.106.L051601

Coupled fission fragment angular momenta

Jørgen Randrup
Nuclear Science Division, Lawrence Berkeley National Laboratory, Berkeley, CA 94720, USA
(Dated: November 4, 2022)

Nuclear fission produces fragments whose spins are coupled to the relative angular motion via angular momentum conservation. It is shown how ensembles of such spins can readily be obained by either direct microcanonical sampling or by sampling of the associated normal modes of rotation. The resulting distribution of the spin-spin opening angle is illustrated in various three- and two-dimensional scenarios and it is demonstrated how recent mutually conflicting model calculations can be well reproduced with different assumptions about the scission geometry.

Introduction. Nuclear fission has become a very active topic, both experimentally [1, 2] and theoretically [2, 3]. In particular, there has recently been considerable interest in the calculation of the correlations between the angular momenta of the fragments and a number of mutually contradictory predictions have been made about the distribution of the spin-spin opening angle, $P_{12}(\psi)$.

The first calculations of $P_{12}(\psi)$ were made with the fission event generator FREYA which assumes that the fragment spins are perpendicular to the fission axis. It was found that, apart from the restriction of being two-dimensional, the spins were nearly independent, in magnitude as well as direction [4, 5]. Accordingly, $P_{12}(\psi)$ exhibited only a small undulation away from constancy.

Subsequently, using time-dependent density functional theory with various energy-density functionals, Bulgac *et al.* [6] found that $P_{12}(\psi)$ exhibits a large angular variation and peaks around $\psi \approx 130^\circ$.

Very recently, dynamical calculations with Antisymmetrized Molecular Dynamics have yielded a nearly symmetric distribution that peaks slightly above 90° [7].

The present situation is thus rather unclear and it is the purpose of this paper to provide a framework within which it can be understood how such widely different results can emerge when the coupled spins are sampled under different assumptions.

First, descriptions are given of two different (but equivalent) general techniques for sampling angular momenta that are subject to conservation relations that render them correlated. Though the methods are applicable generally, the present study concentrates on the sampling of the two fragment spins $\boldsymbol{S}_1$ and $\boldsymbol{S}_2$ together with the angular momentum associated with the relative fragment motion, $\boldsymbol{S}_0$.

Then these methods are applied to the sampling of the three angular momenta, $\{\boldsymbol{S}_i\}$, and it is demonstrated that the two methods do indeed yield identical results. The focus is first on the more general scenario in which the angular momenta are three-dimensional vectors that are constrained only by the conservation laws. Subsequently, the scenario is addressed in which the angular momenta must be perpendicular to the fission axis (as certainly $\boldsymbol{S}_0$ must be by definition), a requirement that effectively reduces the spins to being two-dimensional.

Sampling methods. Generally, the rotational degrees of freedom of the fledging fragments can exchange energy with the remainder of the system. Because the associated rotational energies are typically relatively small in comparison with the internal excitation energy, the nuclear complex effectively acts as an energy reservoir. Therefore, in the present study where the energy is not important, it is assumed that the rotational energies have canonical distributions characterized by the prevailing temperature in the system at scission. By contrast, because no external torques are acting on the fissioning system, its overall angular momentum is conserved. For simplicity and with no bearing on the results, it is assumed that the total angular momentum vanishes, so angular momentum conservation requires $\boldsymbol{S}_1 + \boldsymbol{S}_2 + \boldsymbol{S}_0 = \boldsymbol{0}$.

Below are described two different but equivalent methods for sampling the microcanonical ensemble of the three coupled angular momenta $\{\boldsymbol{S}_i\}$.

An important role is played by the moments of inertia whose relative magnitudes influence the appearance of $P_{12}(\psi)$. For simplicity, the two fragments are treated as solid spheres. Their moments of inertia are denoted by $\mathcal{I}_1$ and $\mathcal{I}_2$ and the numerical calculations use $\mathcal{I}_i = \frac{2}{5} M_i R_i^2$ where M_i is the fragment mass and R_i is its radius. Furthermore, $\mathcal{I}_0 = \mu R^2$ is the moment of inertia associated with the relative motion where $R = R_1 + R_2 + d$ is the distance between the two fragment centers and $\mu = M_1 M_2/(M_1 + M_2)$ is the reduced mass.

Direct microcanonical sampling. The perhaps conceptually simplest method makes a direct sampling of the microcanonical ensemble defined by the total energy E and the total angular momentum.

The fragments are assumed to be non-interacting, so the total rotational energy of the system is given by $E = S_1^2/2\mathcal{I}_1 + S_2^2/2\mathcal{I}_2 + S_0^2/2\mathcal{I}_0$. The expectation value of any spin-dependent "observable", $F\{\boldsymbol{S}_i\}$, is then

$$\langle F\{\boldsymbol{S}_i\}\rangle \;=\; \frac{!}{\Omega_D(E)} \prod_{i=0}^{2} \left[\int d^D \boldsymbol{S}_i\right] F\{\boldsymbol{S}_i\} \\ \times\; \delta(E - \sum_{i=0}^{2} \frac{S_i^2}{2\mathcal{I}_i})\; \delta^{(D)}(\sum_{i=0}^{2} \boldsymbol{S}_i)\;, \qquad (1)$$

where the corresponding microcanonical phase-space vol-

ume for D-dimensional spins is [8]

$$\Omega_D(E) \equiv \prod_{i=0}^{2}\left[\int d^D\boldsymbol{S}_i\right]\,\delta(E-\sum_{i=0}^{2}\frac{S_i^2}{2\mathcal{I}_i})\,\delta^{(D)}(\sum_{i=0}^{2}\boldsymbol{S}_i)$$
$$= \frac{2\pi}{\Gamma(D)}\left(\frac{\mathcal{I}_1\mathcal{I}_2\mathcal{I}_0}{\mathcal{I}}\right)^{D/2}[2\pi E]^{D-1}\,, \qquad (2)$$

with $\mathcal{I}\equiv\mathcal{I}_1+\mathcal{I}_2+\mathcal{I}_0$. Although the total rotational energy E fluctuates in the actual fissioning system, this has no impact when only directional effects are considered. The specific value of E is thus immaterial. The focus is here on the opening angle between the two fragment spins, ψ_{12}, where $\cos\psi_{12}=\boldsymbol{S}_1\cdot\boldsymbol{S}_2/(S_1S_2)$, so the normalized opening-angle distribution $P_{12}(\psi)$ is given by the expectation value of $F\{\boldsymbol{S}_i\}\equiv\delta(\psi_{12}-\psi)$.

The actual evaluation is carried out by sampling the microcanonical distribution. Though this may appear to be a technically demanding task, it can in fact be accomplished remarkably easily [8, 9]: first tentative spin values $\{\boldsymbol{S}_i'\}$ are sampled independently from Boltzmann distributions with a common but arbitrary temperature; then the resulting total angular momentum is calculated, $\boldsymbol{S}'=\boldsymbol{S}_1'+\boldsymbol{S}_2'+\boldsymbol{S}_0'$ and the corresponding rotational frequency is determined, $\boldsymbol{\omega}'=\boldsymbol{S}'/\mathcal{I}$; the overall rotational motion is then removed, yielding $\boldsymbol{S}_i''=\boldsymbol{S}_i'-\mathcal{I}_i\boldsymbol{\omega}'$, and these spins are finally scaled by a common factor $c=\sqrt{E/E''}$ to ensure that the specified total energy E is matched, yielding the spins $\{\boldsymbol{S}_i\}=\{c\boldsymbol{S}_i''\}$. (This last step is of course superfluous when only directional effects are of interest.) The resulting spins clearly satisfy the requirements on the total angular momentum and, crucially, they are distributed according to the correct microcanionical measure (see Refs. [8, 9] for a proof of this key feature). This sampling method is *efficient* (no rejections are required), *robust* (no delicate numerical cancellations occur), and *fast* (millions of samples can be obtained in seconds on a typical laptop).

Sampling of normal modes. An alternative, equivalent, sampling technique utilizes the normal spin modes of the system which are obtained by bringing the rotational energy onto diagonal form,

$$E=\frac{S_1^2}{2\mathcal{I}_1}+\frac{S_2^2}{2\mathcal{I}_2}+\frac{|\boldsymbol{S}_1+\boldsymbol{S}_2|^2}{2\mathcal{I}_0}=\frac{s_+^2}{2\mathcal{I}_+}+\frac{s_-^2}{2\mathcal{I}_-}, \qquad (3)$$

where angular momentum conservation has been used to replace the angular momentum of the relative motion, $\boldsymbol{S}_0$, by $-\boldsymbol{S}_1-\boldsymbol{S}_2$. The moments of inertia of the normal modes are [10]

$$\mathcal{I}_+^{-1}=[\mathcal{I}_1+\mathcal{I}_2]^{-1}+\mathcal{I}_0^{-1}\ ,\ \ \mathcal{I}_-^{-1}=\mathcal{I}_1^{-1}+\mathcal{I}_2^{-1}\ , \qquad (4)$$

where it should be noticed that $\mathcal{I}_+\approx\mathcal{I}_1+\mathcal{I}_2$ when $\mathcal{I}_0\gg\mathcal{I}_1+\mathcal{I}_2$. The components of the normal modes $\boldsymbol{s}_\pm$ may thus be sampled from the respective Boltzmann distributions and the expectation value of an observable $F\{\boldsymbol{S}_i\}$ can be evaluated as

$$\langle F\{\boldsymbol{S}_i\}\rangle=\frac{1}{\Omega_T}\int d^D\boldsymbol{s}_+\int d^D\boldsymbol{s}_-\,F\{\boldsymbol{S}_i\}\,\mathrm{e}^{-E/T}\ , \qquad (5)$$

where E is the rotational energy given in Eq. (3) and the canonical phase space is $\Omega_T=[(2\pi\mathcal{I}_+T)(2\pi\mathcal{I}_-T)]^{D/2}$.

Once the normal spins $\boldsymbol{s}_\pm$ have been sampled, the individual fragment spins can readily be constructed [10],

$$\boldsymbol{S}_1=\frac{\mathcal{I}_1}{\mathcal{I}_1+\mathcal{I}_2}\boldsymbol{s}_++\boldsymbol{s}_-\ ,\quad \boldsymbol{S}_2=\frac{\mathcal{I}_2}{\mathcal{I}_1+\mathcal{I}_2}\boldsymbol{s}_+-\boldsymbol{s}_-\ , \qquad (6)$$

and the orbital angular momentum is $\boldsymbol{S}_0=-\boldsymbol{s}_+$. Thus the conservation of angular momentum is built into the normal modes $\boldsymbol{s}_\pm$, each of which carries no total angular momentum. The mode sampling method has the special advantage that different temperatures can be employed for different modes, thus making it possible to control their relative presence, as was recently exploited [10].

The sampling via normal modes is also efficient, robust, and fast. Importantly, it yields the same ensemble of spins $\{\boldsymbol{S}_i\}$ as the direct microcanonical sampling described above, provided that the energy E in Eq. (1) is sampled from the appropriate canonical distribution for three coupled D-dimensional spins, $P(E)\sim E^{D-1}\exp(-E/T)$.

Spin-spin opening-angle distributions. The above sampling methods are now applied to the calculation of the distribution of the opening angle between the fission fragment angular momenta for various scenarios of current interest.

Three-dimensional spins. In the scenario considered here, the three angular momenta involved are three-dimensional, *i.e.* $D=3$, so one may write $\boldsymbol{S}_i=(S_i^x,S_i^y,S_i^z)$.

First, to establish a convenient reference scenario, the two fragment spins are sampled entirely independently from isotropic distributions, such as Boltzmann distributions, $P(\boldsymbol{S}_i)\sim\exp(-S_i^2/2\mathcal{I}_iT_i)$, where the values of the temperature parameters T_i are immaterial. The directions of the fragment spin vectors are then distributed uniformly over 4π and it follows that the distribution of $\cos\psi$ is constant, equivalent to the opening angle itself having the distributon $P_{12}^{\mathrm{indep}}(\psi)\sim\sin\psi$.

In reality the fragments are interacting and their spins are coupled to the angular momentum of their relative motion, $\boldsymbol{S}_0$. Because the combined system is isolated, its total angular momentum remains unchanged and so the appropriate statistical spin distribution has a microcanonical form.

Another reference scenario is the simple (but unrealistic) case where the two fragments are equal in size and are touching; the ratios of their moments of inertia are then $\mathcal{I}_1:\mathcal{I}_2:\mathcal{I}_0=1:1:5$. The resulting opening-angle distribution, $P_{12}^{\mathrm{touch}}(\psi)$, is displayed in Fig. 1. The coupling causes it to be skewed away from symmetry and it peaks near $\psi=110^\circ$. The figure also illustrates that $P_{12}(\psi)$ is generally not very sensitive to the mass asymmetry.

The touching-sphere scenario is not realistic because the distance between the fragment centers exceeds the sum of the two fragment radii at the time of their formation, as indicated by the measured fragment kinetic ener-

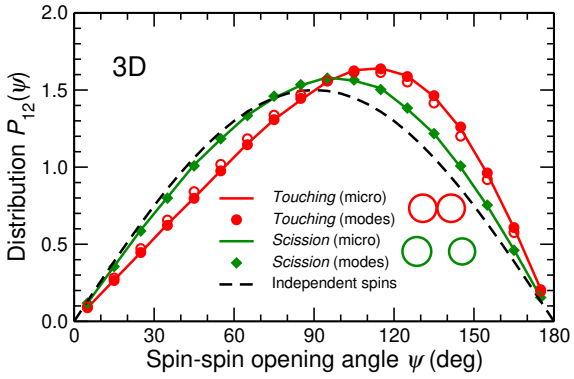


FIG. 1: The distribution of the fragment spin opening angle ψ obtained by 3D sampling in various scenarios: *Touching:* A schematic reference scenario of two touching spheres of equal size in which case the relative sizes of the moments of inertia are $\mathcal{I}_1 : \mathcal{I}_2 : \mathcal{I}_0 = 1 : 1 : 5$; *Scission:* A more realistic scenario typical of scission for which the moments of inertia have ratios similar to those used in FREYA (see Table I); and *Independent:* The limiting scenario for large $\mathcal{I}_0$ where the angular momentum constraint is ineffective and the two fragment spins become independent. Each curve is based on one million spin triplets, obtained either by direct microcanonical sampling or by sampling of the normal modes. The opening-angle distribution obtained for $\mathcal{I}_1 : \mathcal{I}_2 : \mathcal{I}_0 = 0.5 : 1.5 : 5$ is also shown (open circles).

gies. (In model calculations, the center separation typically exceeds the sum of the fragment radii by $d = 4$ fm.) As a consequence, the moment of inertia for the relative motion at scission exceeds those of the individual fragments by over an order of magnitude (whereas the individual moments of inertia are of comparable size). In order to approximate such a scenario for illustrative purposes, the employed moments of inertia are similar to those used in FREYA, see Table I, but the present results are not very sensitive to the precise values. [It should be noted that [1]) the moments of inertia employed in FREYA lead to a reasonable reproduction of the overall fragment spin distribution [5] and [2]) only the *relative* sizes of the moments of inertia are needed for the present study.]

Case	$\mathcal{I}_1/\bar{\mathcal{I}}$	$\mathcal{I}_2/\bar{\mathcal{I}}$	$\mathcal{I}_0/\bar{\mathcal{I}}$
^{235}U($n_{\rm th}$,f)	0.71	1.29	16.91
^{239}Pu($n_{\rm th}$,f)	0.73	1.27	17.02
^{252}Cf(sf)	0.77	1.23	17.08
This work	0.75	1.25	17

TABLE I: The average values of the moments of inertia used by the fission event generator FREYA [11], relative to the mean fragment moment of inertia $\bar{\mathcal{I}} = (\mathcal{I}_1 + \mathcal{I}_2)/2$. The last line shows the ratios used here to illustrate scission.

The resulting opening-angle distribution, $P_{12}^{\rm sciss}(\psi)$, is closer to the limiting uncorrelated form than touching spheres, reflecting the fact that the coupling to the relative motion becomes less effective as the associated moment of inertia $\mathcal{I}_0$ is increased.

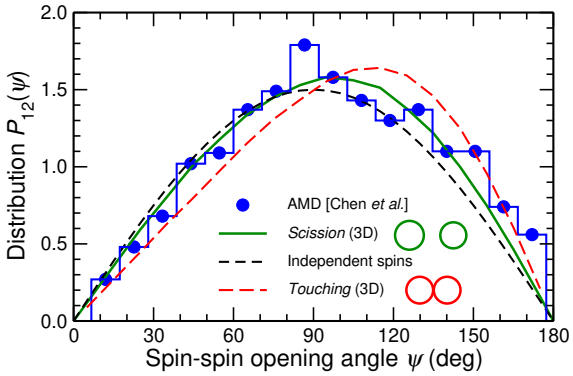


FIG. 2: Thw opening-angle distribution obtained by Chen, Ishizuka, and Chiba [7] with Anti-symmetrized Molecular Dynamics for fission of ^{252}Cf are compared with the 3D sampling results for the *scission* scenario, $P_{12}^{\rm sciss}(\psi)$, shown in Fig. 1.

It is interesting that this distribution quite closely resembles the one obtained by recent AMD simulations of fission of ^{252}Cf [7], as shown in Fig. 2. Antisymmetrized Molecular Dynamics represents the state of the system by a Slater determinant of Gaussian wave packets whose centroids are propagated by classical equations of motion with the potential energy having been augmented by the repulsive effect of the antisymmetrization. This implies a short mean free path for the individual centroids and a rapid local equilibration might therefore be expected. This appears to be indeed borne out by the AMD results for the distribution of the spin-spin opening angle which are consistent with the 3D equilibrium form in Fig. 1.

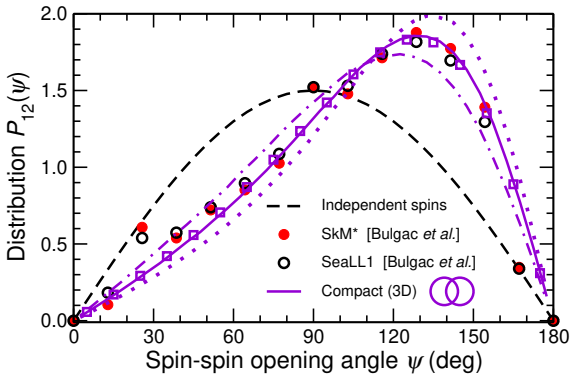


FIG. 3: The opening-angle distributions calculated by Bulgac *et al.* [6] for ^{252}Cf(sf) with time-dependent density functional theory using either the SkM* or the SeaLL1 energy density functional are compared with 3D sampling results for a *compact* scenario for which $\mathcal{I}_1 : \mathcal{I}_2 : \mathcal{I}_0 = 1 : 1 : 2$. To illustrate the sensitivity to $\mathcal{I}_0$ are also shown the distributions for a 50% smaller (dots) or a 50% larger (dot-dash) $\mathcal{I}_0$ value. The open squares show the results for $\mathcal{I}_1 : \mathcal{I}_2 : \mathcal{I}_0 = 0.75 : 1.25 : 2$.

It is also noteworthy that the results obtained for

$P_{12}(\psi)$ by Bulgac *et al.* [6] using time-dependent density functional theory can be well reproduced by 3D samplings that employ the ratios $\mathcal{I}_1 : \mathcal{I}_2 : \mathcal{I}_0 = 1 : 1 : 2$, as shown in Fig. 3. It is quite remarkable that such a good agreement can be obtained by using a moment of inertia for the relative motion that is just the sum of the two individual moments of inertia, a value that is only 40% of that for touching spheres (about an order of magnitude below those for typical scission configurations) and corresponds to the two fragments overlapping significantly.

To provide a sense of how well determined the relative value of $\mathcal{I}_0$ is, Fig. 3 also shows the distributions obtained with $\mathcal{I}_0$ values that are either 50% smaller (*i.e.* 1:1:1) or 50% larger (*i.e.* 1:1:3). Neither one of those distributions comes close to reproducing the results from Ref. [6]. Thus it appears that the optimal value is rather narrowly determined to be $\mathcal{I}_0 \approx \mathcal{I}_1 + \mathcal{I}_2$.

Two-dimensional spins. It is theoretically expected [10, 12], as well as experimentally indicated [13, 14], that the fission fragment angular momenta are predominantly perpendicular to the fission axis. It is therefore of interest to also analyze idealized scenarios where the fragment spins are perfectly perpendicular to the fission axis. Such a situation is analogous to the above case, except that the dimensionality is now only $D = 2$, so $\boldsymbol{S}_i = (S_i^x, S_i^y, 0)$. Figure 4 shows the spin-spin opening angle distribution for the same instructive 2D scenarios as shown in Fig. 1.

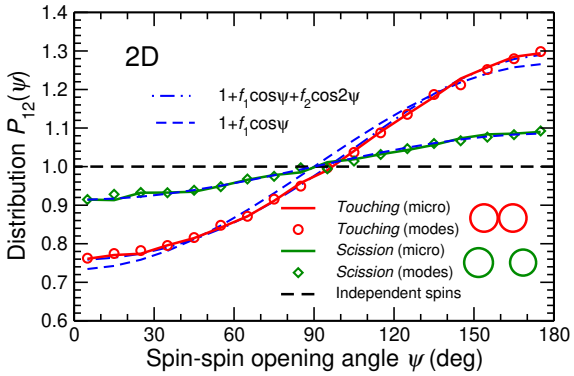


FIG. 4: The distribution of the fragment spin opening angle ψ obtained by 2D sampling of the three angular momenta, using moments of inertia corresponding either to *touching* ($\mathcal{I}_1 : \mathcal{I}_2 : \mathcal{I}_0 = 1 : 1 : 5$) or to *scission* ($\mathcal{I}_1 : \mathcal{I}_2 : \mathcal{I}_0 = 0.75 : 1.25 : 17$). The samplings were done either microcanonically or via the normal modes. The two dashed curves are the corresponding first-order Fourier fits, while the dot-dashed curve is the second-order Fourier fit to the touching-sphere distribution which has a larger amplitude.

In the reference scenario of totally independent spins, $\mathcal{I}_0/\bar{\mathcal{I}} \to \infty$, the directions of the fragment spin vectors are distributed uniformly in the perpendicular plane and it follows that the distribution of the opening angle ψ is constant.

When the coupling to the orbital motion is taken into account in the sampling, the two fragment spins have a slight preference for being directed oppositely, The opening-angle distribution is typically well represented by the lowest-order Fourier approximation, $P_{12}(\psi) \sim 1 + f_1 \cos\psi$. When scission moments of inertia are used the deviation from uniformity is fairly small, $f_1 = -0.086$.

As was the case in 3D, the touching-sphere configuration, with its considerably smaller $\mathcal{I}_0$, leads to larger deviations of $P_{12}(\psi)$ from the independent scenario, namely $f_1 = -0.264$, and so the second-order Fourier term is required for an accurate representation, $P_{12}^{\rm touch}(\psi) \sim 1 + f_1 \cos\psi + f_2 \cos 2\psi$, with $f_2 = 0.028$, as is apparent from Fig. 4.

The standard version of the fission model FREYA [15] assumes that the fission fragments emerge with angular momenta that are perpendicular to the fission axis and they are therefore sampled from the corresponding 2D distribution. The resulting spin-spin opening-angle distribution [4] is then in accordance with the results sampled here, as shown in Fig. 5.

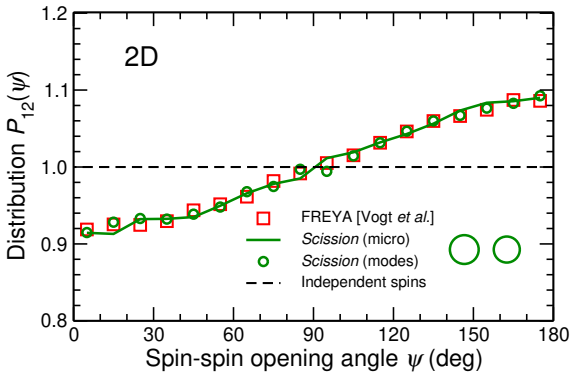


FIG. 5: The distribution of the fragment spin opening angle ψ obtained with FREYA for ^{235}U(n,f) [4] is compared with the 2D sampling results for the *scission* scenario shown in Fig. 4.

Concluding remarks. This study describes two different but equivalent methods for sampling angular momenta that are correlated due to conservation laws. These methods were applied to sampling the angular momenta of fission fragments in either three or two dimensions. With a focus on the distribution of the spin-spin opening angle ψ, it was illustrated how the relative magnitude of the moment of inertia for the orbital fragment motion influences $P_{12}(\psi)$ significantly.

Comparisons with recent model calculations of the opening-angle distribution showed that the result obtained with Antisymmetrized Molecular Dynamics [7] agrees well with the statistical form pertaining to 3D spins with moments of inertia typical of scission, as might be expected. On the other hand, it is puzzling that results obtained with microscopic time-dependent functional theory [6] can be reproduced with the 3D equilibrium distribution using a relative moment of inertia that corresponds to a shape that is significantly more compact than touching spheres. It may be noted that the 3D samplings do not invoke the scission geometry and thus

ignores the basic geometric requirement that the relative angular momentum be perpendicular to the fission axis.

Finally, it was shown that the 2D equilibrium form with scission moments of inertia reproduces the results of fission simulations with the FREYA code [4, 5] which does take account of the specific scission geometry and generates fragment spins that are perpendicular to the fission axis.

The present analysis brings out an important feature of the coupled angular momenta appearing in fission: The relative motion, due to the large size of the associated moment of inertia in comparison with those of the individual fragments, effectively acts as a reservoir of angular momentum. Then the conservation of angular momentum has little effect on the fragment spins and they become nearly independent. Indeed, the angular momenta generated by FREYA are only slightly correlated with regard to both their directions and their magnitudes. The latter feature was recently observed experimentally [16].

In view of the large differences between the model calculations of the spin-spin opening angle distribution, experimental information on this observable is highly desirable as it could help to clarify the scission physics.

Acknowledgments. I thank R. Vogt for helpful discussions and comments on the manuscript, and I also wish to acknowledge communications with T. Døssing, L. Sobotka, and J. Wilson. This work was supported by the Office of Nuclear Physics in the U.S. Department of Energy's Office of Science under Contract No. DE-AC02-05CH11231; it was stimulated by the Worshop on Fission Fragment Angular Momenta recently hosted by A. Bulgac at the University of Washington in Seattle, June 21-24, 2022.

[1] A.N. Andreyev, K. Nishio, and K.-H. Schmidt, Nuclear fission: a review of experimental advances and phenomenology, Rep. Prog. Phys, **81**, 016301 (2018).

[2] K.-H. Schmidt and B. Jurado, Review on the progress in nuclear fission -— experimental methods and theoretical descriptions, Rep. Prog. Phys, **81**, 106301 (2018).

[3] M. Bender *et al.*, Future of nuclear fission theory, J. Phys. G. Nucl. Part. Phys. **47**, 113002 (2020).

[4] R. Vogt and J. Randrup, Angular momentum effects in fission, Phys. Rev. C **103**, 014610 (2021).

[5] J. Randrup and R. Vogt, Generation of fragment angular momentum in fission, Phys. Rev. Lett. **127**, 062502 (2021).

[6] A. Bulgac, I. Abdurrahman, K. Godbey, and I. Stetcu, Fragment intrinsic spins and fragments' relative orbital angular momentum in nuclear fission, Phys. Rev. Lett. **128**, 022501 (2021).

[7] J. Chen, Master thesis at Tokyo Institute of Technology, May 2022; presented at the Workshop on Fission Fragment Angular Momenta held at the University of Washington, Seattle, June 21-24, 2022 [https://indico.in2p3.fr/event/26459], J. Chen, C. Ishizuka, and S. Chiba, to be published.

[8] J. Randrup, Microcanonical sampling of momenta in simulations of many-particle systems, Comp. Phys. Comm. **59**, 439 (1990).

[9] J, Randrup. Microcanonical sampling of momenta, Nucl. Phys. A **522**, 651 (1991).

[10] J. Randrup, T. Døssing, and R. Vogt, Probing fission fragment angular momenta by photon measurements, Phys. Rev. C **106**, 014609 (2022).

[11] J. Randrup and R. Vogt, Calculation of fission observables through event-by-event simulation, Phys. Rev. C **80**, 024601 (2009).

[12] T. Døssing and J. Randrup, Dynamical evolution of angular momentum in damped nuclear reactions: (I) Accumulation of angular momentum by nucleon transfer, Nucl. Phys. A **433**, 215 (1985).

[13] J.B. Wilhelmy, E. Cheifetz, R.C. Jared, S.G. Thompson, H.R. Bowman, and J.O. Rasmussen, Angular momentum of primary products formed in the spontaneous fission of ^{252}Cf, Phys. Rev. C **5**, 2041 (1972).

[14] A. Wolf and E. Cheifetz, Angular distributions of specific gamma rays emitted in the deexcitation of prompt fission products of ^{252}Cf, Phys. Rev. C **13**, 1952 (1976).

[15] J. Randrup and R. Vogt, Refined treatment of angular momentum in the event-by-event fission model FREYA, Phys. Rev. C **89**, 044601 (2014).

[16] J. Wilson *et al.*, Angular momentum generation in nuclear fission, Nature (London) **590**, 566 (2021).